LA-UR-16-25562
Approved for public release; distribution is unlimited.

Title: A New Multiphase Equation of State for Composition B

Author(s): Coe, Joshua Damon
Margevicius, Madeline Alma

Intended for: Report

Issued: 2016-07-26

A New Multiphase Equation of State for Composition B

Joshua D. Coe[a)] and Madeline A. Margevicius
Theoretical Division, Los Alamos National Laboratory, Los Alamos, NM, 87545

(Dated: 25 July 2016)

We describe the construction of a complete equation of state for the high explosive Composition B in its unreacted (inert) form, as well as chemical equilibrium calculations of its detonation products. The multiphase reactant EOS is of SESAME type, and was calibrated to ambient thermal and mechanical data, the shock initiation experiments of Dattelbaum, et al., and the melt line of trinitrotoluene (TNT).

I. INTRODUCTION

Composition B ("Comp B", hereafter) is a high explosive (HE) heavily utilized by the United States and other allied nations from World War II to the present. Its composition has been reported in various ways, but most commonly as a mixture of 59.5% RDX, 39.5% TNT, and 1% wax by weight. Dobratz[1] lists the composition as 63:36:1, a formulation known as "LASL Comp B" or "Classic Comp B". This results from skimming off molten TNT during melt casting, a process known as "richening". Without the wax, the 60:40 mixture is known as Comp B-3.[a] All can be either be pressed or cast.

Herein we describe the construction of a multiphase equation of state (EOS) for inert Comp B, in addition to chemical equilibrium calculation of its detonation products. The EOS is produced in the form of SESAME table[2–4] 95500. The table is a tensor product grid of pressure, energy, and Helmholtz free energy as functions of temperature and density. We describe our methodology in some detail in the following section, then compare our results with those of experiment.

II. THEORY

The first matter to resolve was that of chemical composition. Dobratz lists the 63:36:1 and 60:40 mixtures as $C_{2.03}H_{2.64}N_{2.18}O_{2.67}$ and $C_{2.05}H_{2.51}N_{2.15}O_{2.67}$, respectively. In order to estimate the wax component, we calculated the theoretical composition of a 63.5:36.5 mix of RDX:TNT, then normalized to the Dobratz values based on the assumption that the wax is nitrogen-free[b]. This gave a wax contribution of $C_{0.05}H_{0.14}$. We then simply added this (without renormalizing) to the 60:40 mix. This yielded $C_{2.10}H_{2.65}N_{2.15}O_{2.67}$, having a mean atomic weight and number of A=10.53 g/mol and Z=5.40e, respectively. The molecular weight (MW) was determined according to $0.6MW_{RDX}+0.4MW_{TNT}$=224.124 g/mol, based on the MWs of RDX and TNT. Data have been reported for Comp B over a range of initial densities, but we chose as our reference ρ_{ref}=1.713 g/cc, one typical of melt-casting under vaccuum. This is very close to the nominal density of 1.71 g/cc recorded in Dobratz, but somewhat less than the theoretical maximum value of 1.742 g/cc.

$$\begin{gathered}\text{composition} = C_{2.10}H_{2.65}N_{2.15}O_{2.67}\\ \bar{Z} = 5.40\\ \bar{A} = 10.53 \text{ g/mol}\\ \rho_{ref}=1.713 \text{ g/cc}\end{gathered}$$

TABLE I. The basic EOS parameters.

A. Inert EOS

The inert EOS was based on the following decomposition of the Helmholtz free energy[2–4]

$$F(\rho,T) = \phi(\rho) + F_{ion}(\rho,T) + F_{elec}(\rho,T). \qquad (1)$$

The first term on the rhs is the energy of the static lattice at 0K, where all ions and electrons are in their ground state. This "cold curve" is not equivalent to the zero temperature isotherm, as it does not include zero point energy (zpe). The second term is the free energy of ionic excitations with electrons in their ground state, and the last is the free energy of electronic excitations with the ions in their ground state. In order for the model to be complete, there should be an additional term coupling the ions with the electrons; this coupling is assumed to be small, and so we will neglect it. All other thermodynamic potentials may be obtained by Legendre transformation of (1), and various observables found by application of appropriate derivatives. For instance, the internal energy is

$$E = F - T\left(\frac{\partial F}{\partial T}\right)_{\rho}, \qquad (2)$$

and the pressure is

$$P = \rho^2\left(\frac{\partial F}{\partial \rho}\right)_{T}. \qquad (3)$$

Eqn. (1) thus constitutes as complete a description of a material as classical thermodynamics can provide. The

a)Electronic mail: jcoe@lanl.gov

[a] To make matters more confusing, Comp B is frequently described - nonsensically - as 60% RDX, 40% TNT, and 1% wax.

[b] We were unable to find anything going by the name of "wax" whose composition included nitrogen.

`OpenSesame` package was used to build the inert EOS. We express otherwise extensive quantities (e.g., E, V, and S) in specific units throughout.

1. Cold Curve

The cold curve comprises three different models joined at user-defined compressions $\eta_{\rm lo}$ and $\eta_{\rm hi}$, where we are defining compression as $\eta = \rho/\rho_{\rm ref}$. In expansion, the cold energy was assigned a "Lennard-Jones" form,

$$\phi(\rho) = a_1\rho^{a_2} - a_3\rho^{a_4} + E_0. \tag{4}$$

We supplied values for a_4 and the cohesive energy $E_{\rm coh}$, which is related to E_0 through

$$E_0 = E_{\rm coh} + \phi(\rho_{\rm min}). \tag{5}$$

$\rho_{\rm min}$ is the density at which ϕ obtains its minimal value. Parameters a_1-a_3 were then adjusted automatically to ensure continuity of the energy and its first two density derivatives at the match point $\eta_{\rm lo}$.[5]

For low to moderate compressions (essentially defined as the regime where there were data), we used a Vinet-Rose form

$$\phi(\rho) = \phi_* + 4\frac{B_*}{\rho_*}(B'_* - 1)^{-2}[1 - (1+x)e^{-x}]^{-1}, \tag{6}$$

where

$$x = \frac{3}{2}\left(B'_* - 1\right)\left[\left(\frac{\rho_*}{\rho}\right)^{\frac{1}{3}} - 1\right]. \tag{7}$$

At high compressions (beyond the domain of the data), the cold curve was described using Thomas-Fermi-Dirac (TFD) theory.[6–8] Because TFD contains no free parameters, an interpolant function was required,

$$Y(\rho) = 1 + \frac{b_1}{\rho} + \frac{b_2}{\rho^{4/3}}, \tag{8}$$

such that for $\eta > \eta_{\rm hi}$,

$$\phi(\rho) = [\phi_{TFD}(\rho) - \phi_{TFD}(\rho_{\rm hi})]Y(\rho) + \Delta E_c. \tag{9}$$

Here, $\rho_{\rm hi} = \rho_{\rm ref}\eta_{\rm hi}$. Analogous to the L-J model, parameters b_1, b_2, and ΔE_c were varied to ensure continuity of the energy, pressure, and bulk modulus at the match point $\eta_{\rm hi}$.

2. Thermal Models

A Debye model was used for F_{ion} of the solid. Because this model is well-canvassed in numerous sources,[9] we highlight only a couple of its features. The first is that it contains a single parameter, the Debye temperature (Θ_D) at the reference density. The Debye model is purely harmonic as well, such that in order to extract a thermal pressure one must resort to the quasiharmonic approximation.[10] Here, anharmonic effects are folded in through the density-dependence of the lattice frequencies (or in the case of a simplified model like Debye, *the* characteristic frequency), itself introduced via the the Grüneisen parameter Γ. Γ is defined as

$$\Gamma(\rho) = \left(\frac{\partial \ln T}{\partial \ln \rho}\right)_S, \tag{10}$$

which can under mild assumption[c] be shown equivalent to[11]

$$\Gamma(\rho) = \left(\frac{\partial \ln \Theta_D}{\partial \ln \rho}\right)_T. \tag{11}$$

We used the following form for Γ,

$$\Gamma(\rho) = \begin{cases} \Gamma_\infty + g_1(\frac{\rho_g}{\rho}) + g_2(\frac{\rho_g}{\rho})^2, & \rho \geq \rho_g \\ \Gamma_0 + g_3(\frac{\rho}{\rho_g}) + g_4(\frac{\rho}{\rho_g})^2\ , & \rho \leq \rho_g, \end{cases} \tag{12}$$

which in combination with (11) provides a simple ODE that can be integrated to obtain $\Theta_D(\rho)$. This leads to

$$P_{ion} = \rho\Gamma E_{ion}. \tag{13}$$

We provided values for Γ_∞, Γ_0, and the left and right ρ derivatives of Γ, leaving four equations in the four unknowns g_1-g_4. These were adjusted to ensure continuity of Γ and recovery of the specified derivative values at the match point ρ_g.

One of the distinctive features of TNT is its low melting point of 353 K (80 °C), much lower than that of RDX (205 K, or 478 °C). It is well known that melting of the TNT component produces a heterogeneous mixture. We did not attempt to capture this complexity, but modeled Comp B above the TNT melt line as a homogeneous fluid. For this we used a model inspired by the vibration-transit theory of liquids.[12] We refer the interested reader to Ref. 13, and pause only to note that the sole input required was the entropy change upon melting (ΔS). We

$$\begin{gathered} a_4 = 1.0 \\ E_{\rm coh} = 120 \text{ kcal/mol} \\ \eta_{\rm lo} = 0.98 \\ \phi_* = 0 \\ \rho_* = 1.881 \text{ g/cc} \\ B_* = 26.705 \text{ GPa} \\ B'_* = 7.0 \\ \eta_{\rm hi} = 2.0 \end{gathered}$$

TABLE II. Inputs used to define the cold curve.

[c] In particular, that the entropy be an explicit function of a scaled temperature.

$\Theta_D(\rho_{\rm ref})$ = 1272 K
ρ_m =1.55 g/cc
$T_m(\rho_m)$ = 353.5 K
ΔS = 0.8 k_B/atom
ρ_g = 1.713
$\Gamma(\rho_g)$ = 0.84
Γ_0 = 1.0
Γ_∞ = 0.6667
$\frac{d\Gamma}{d\ln\rho}(\rho_g)$ = -2.9

TABLE III. Inputs used to define the nuclear model. The left and right density derivatives of Γ were the same.

treated Comp B as a "normal" melter, meaning its electronic structure fails to undergo significant change upon passage to the liquid. This results in a value of $\Delta S = 0.8$ R per mol.

The melt line was of Lindemann form,

$$\frac{T_m(\rho)}{T_m(\rho_m)} = \left(\frac{\rho}{\rho_m}\right)^{-2/3}\left[\frac{\theta(\rho)}{\theta(\rho_m)}\right]^2, \qquad (14)$$

requiring specification of the melt temperature (T_m) and density (ρ_m) at ambient pressure. The melt temperature chosen was that of TNT, but the melt density was set somewhat arbitrarily.

Because Comp B is an insulator, thermal electronic contributions were neglected for the solid. But in order for the table to possess the correct limiting behavior at low ρ and high T, TFD was included for the liquid.

3. Multiphase Construction

Due to the low melt temperature of TNT, the inert required an explicitly multiphase treatment. The algorithm reads in the 301 (total) tables for each phase. It then adjusts the mass fractions and partial volumes until phases are in pressure equilibrium and the Gibbs free energy of the full mixture is minimized. Additional control may be exercised through "windowing": defining domains of density or temperature in which various phases are excluded *a priori*. In addition to a new 301 table, this procedure produces the 321 table listing the mass fractions. Additional details on this, and the construction of the melt tables 411 and 412, can be found in Ref. 14.

B. Products EOS

Because Comp B (like any explosive) undergoes massive chemical change upon decomposition, it was necessary to treat its reaction products as a material distinct from the HE itself. This called for an alternate theoretical approach. Detonation loci were generated using the High Explosive Equation of State (`HEOS`) code[15] by direct solution of the jump condition, equation (17) below.

TABLE IV. EXP6 parameters for fluids included in the decomposition products mixture.

Component	$r_0/\mathring{A}$	(ϵ/k_B)/K	α
N_2	4.0876	128.24	12.936
N_2O	4.096	335.0	13.781
CO_2	4.096	335.0	13.781
H_2O	3.5	424.0	10.0
CO	4.0876	128.24	12.936
C_2N_2	4.9	330.0	13.0
CH_4	4.22	154.1	12.5
H_2	3.43	36.4	11.1
HCO_2H	4.096	335.0	13.781

Products were modeled as an ideal mixture[16] of fluids and solid carbon clusters. The fluid mixture comprised N_2, CO, CO_2, H_2O, H_2, N_2O, C_2N_2, CH_4, and HCOOH. Its free energy was calculated as follows

$$G_{\rm mix}(P,T,\mathbf{x}) = \sum_{i=1}^{N} x_i G_i^0(P,T) + RT\sum_{i=1}^{N} x_i \ln x_i, \quad (15)$$

where $N = 9$ is the number of mixture components, each having mass fraction x_i. The second sum on the rhs is the free energy of mixing (purely entropic in an ideal mixture), while the first is that of the isolated fluids. The free energy of each fluid component i, G_i^0, was calculated using Ross perturbation theory[17] based on an EXP6 potential.[18] The latter has the form

$$\phi(r) = \frac{\epsilon}{\alpha - 6}\left[6e^{-\alpha\left(\frac{r}{r_0}-1\right)} - \alpha\left(\frac{r_0}{r}\right)^6\right], \qquad (16)$$

where α sets the steepness of the repulsive wall, ϵ represents the energetic well depth, and r_0 gives the separation at which the intermolecular potential is minimized. EXP6 parameters for each species were calibrated to shock data on the pure fluid,[15] and are listed in Table IV.

Solid carbon was treated as a cluster of 5000 core atoms capped by surface groups N, C+H, and C+O. Description of the surface models can be found elsewhere.[19] The EOS of the cluster core (ρ_0=3.5 g/cm^3) was of Mie-Grüneisen form[20] ($\Gamma = 0.9$) comprising a Murnaghan[21] cold curve (B_0 = 510 GPa, $N = 3.5$)[22] and a Debye thermal ionic contribution (θ_D = 2200K). As a good insulator, diamond's thermal electronic contributions to the free energy were neglected over the domain of interest. As is common practice,[23] $\rho\Gamma$ was assumed constant. The free energy of the complete mixture (fluids+solid) was minimized as a function of chemical composition ($\mathbf{x}$) subject to conservation and non-negativity of elemental mole fractions.

It is important to note that the detonation locus was obtained by solving a jump equation,

$$E - E_0 = \frac{1}{2}(P_0 + P_1)(V_0 - V_1), \qquad (17)$$

in which the initial state was that of the inert and the final that of the equilibrium products mixture. We did this by solving (17) for temperature at a given pressure, assuming an initial state defined by (V_0, E_0) at $P_0 \approx 0$. Dobratz gives a HOF of 1.0 kcal/mol relative to stable elements at $\rho = 0$ and STP. The zero of energy in HEOS is stable elements at $\rho = 0$ and $T = 0$, meaning a correction ΔH had to be applied in order to account for the energy needed to heat the isolated elements up from zero to ambient temperature. This information was taken from the JANAF tables,[24] and was incorporated as follows

$$\begin{aligned}\Delta H &= 0.6(3\Delta H_{\mathrm{C}} + 3\Delta H_{\mathrm{H_2}} + 3\Delta H_{\mathrm{N_2}} + 3\Delta H_{\mathrm{O_2}}) + \\ &\quad 0.4\left(7\Delta H_{\mathrm{C}} + \frac{5}{2}\Delta H_{\mathrm{H_2}} + \frac{3}{2}\Delta H_{\mathrm{N_2}} + 3\Delta H_{\mathrm{O_2}}\right) \\ &= 0.6[3(0.2512) + 3(2.024) + 3(2.072) + 3(2.075)] + \\ &\quad 0.4\left[7(0.2512) + \frac{5}{2}(2.024) + \frac{3}{2}(2.072) + 3(2.075)\right] \\ &= 18.02 \quad \text{kcal/mol} \end{aligned} \tag{18}$$

Thus, E_0 for the solid was 19.02 kcal/mol. This figure was adjusted accordingly for LASL Comp B, but no distinction was made between Comp B and Comp B-3 in this regard.

The liquid was slightly more complicated, in that its E_0 should include the enthalpy change upon heating from T_0 to T_{m}, as well as the latent heat of fusion. For heating at constant pressure, the enthalpy change is simply

$$H(T_m) = H(T_{\mathrm{ref}}) + \int_{T_{\mathrm{ref}}}^{T_m} C_p(T)dT. \tag{19}$$

We evaluated this by numerical integration of our inert EOS result, yielding a value of 6 kcal/mol. The heat of fusion $\Delta H_f = 5.075$ kcal/mol was taken from Ref. 25, resulting in a total E_0 for the liquid of 30.1 kcal/mol.

III. RESULTS

Cold curve and thermal ionic parameters were varied to recover ambient property values, the Hugoniot, and the TNT melt line. A summary of ambient properties as predicted by the inert are compared with experiment in Table V. Agreement is good in all cases, the average and maximum errors both being $< 1\%$. The value of c_0 is that taken from a linear $U_s - u_p$ fit,[26] meaning it is most likely a little high.[20] We also caution that past measurements of the volumetric expansion coefficient (β) and isobaric specific heat (C_p) have yielded wildly different values, and that our selection of those given in Dobratz is somewhat arbitrary.

Figure 1 shows the inert Hugoniot and detonation locus of Comp B ($\rho_0 = 1.713$ g/cc) in the detonation velocity-particle velocity ($D - u_p$) plane. Agreement of our inert EOS with the initiation data of Dattelbaum, et al.[26] is good. The minimum in $D(u_p)$ provides an estimate of the detonation speed at the Chapman-Jouget (CJ) state[27] (D_{CJ}), and on this basis we predict a value of 7.86 km/s. This is lower than the 7.92 km/s listed in Dobratz, as is to be expected given the higher percentage of RDX in the 63:36:1 mixture reported there. We plot the same results in $P - V$ in Figure 2, as well as the Rayleigh line (centered at ρ_{ref}) tangent to the products locus. The combination of our EOS predict von Neumann spike and CJ pressures of 40.1 GPa and 28.9 GPa, respectively.

The TNT melt line was recently measured to high accuracy by Dattelbaum, et al.[28] We compare these data with 95500 results in Figure 3. Once again we find good

TABLE V. Comparison of ambient properties predicted by SESAME 95500 with those obtained from experiment. Agreement is excellent in all cases, with mean and maximum errors of less than 1%. Experimental results were taken from Dobratz. The measured value of Γ was based on that of $\beta B_S/\rho C_P$.

	Measured	EOS
ρ_0 (g/cc)	1.713	1.713
C_P (kJ/kg/K)	1.13	1.13
C_V (kJ/kg/K)	1.09	1.09
c_0 (km/s)	2.41	2.41
B_S (GPa)	9.949	9.948
B_T (GPa)	9.556	9.556
β (K^{-1})	1.64E-4	1.64E-4
Γ (unitless)	0.842	0.840

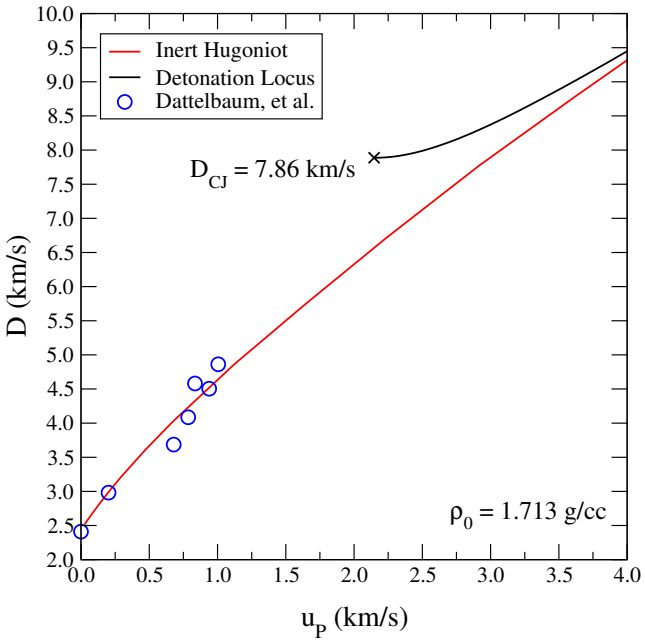

FIG. 1. The inert Hugoniot and detonation locus of Comp B ($\rho_0 = 1.713$ g/cc) as predicted by SESAME 95500 and chemical equilibrium calculation. Experimental uncertainties in the shock initiation data[26] are smaller than the symbol sizes. We predict a CJ detonation speed of 7.86 km/s based on the minimum in $D(u_p)$.

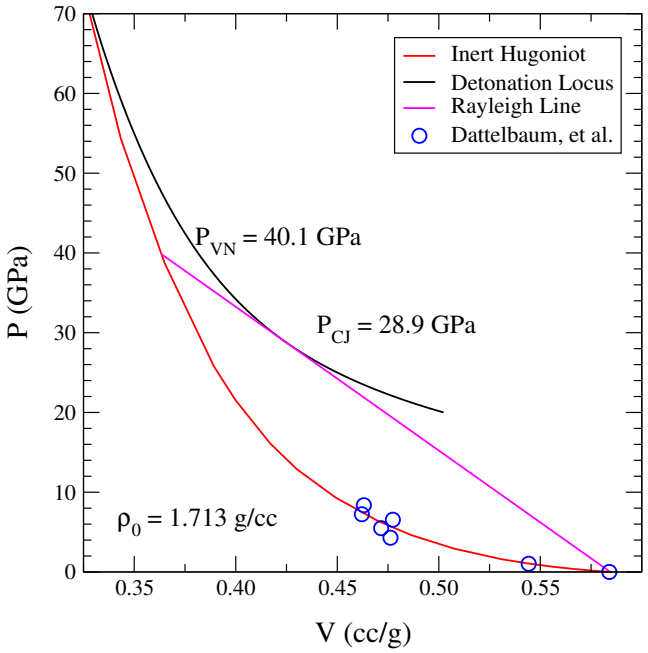

FIG. 2. The inert Hugoniot and detonation locus of Comp B (ρ_0=1.713 g/cc) as predicted by SESAME 95500 and chemical equilibrium calculation. Experimental uncertainties in the shock initiation data[26] are smaller than the symbol sizes. Pressures of the von Neumann spike and CJ state are also indicated.

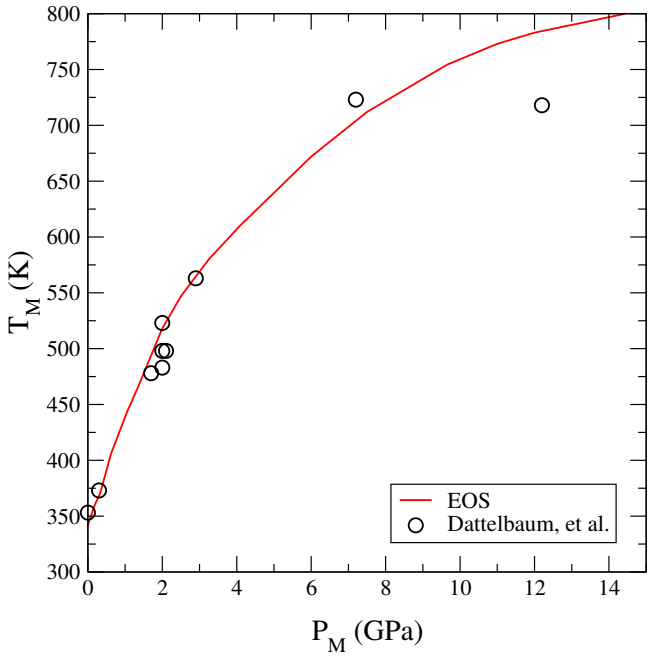

FIG. 3. The melt line of TNT as predicted by SESAME 95500. Experimental uncertainties in the melt data[28] are smaller than the symbol sizes. It is unclear whether the two data points at highest pressure are melted, chemically decomposed, or some combination thereof.[28]

agreement, particularly at lower pressures. It was impossible to determine whether the two points at higher pressure (where agreement with our EOS is not as good) were melted, chemically decomposed, or some combination.[28] As has been noted,[28] the melt line is quite steep (∼80 K/GPa). At this point we reiterate that this is the melt line of pure TNT, and that its precise relation to constitutive properties of Comp B is not straightforward.

Figure 4 gives the phase diagram of the inert in the $P-T$ plane, with the Hugoniot superimposed. As can be seen, SESAME 95500 predicts that the von Neumann spike crosses the melt line. In principle this would suggest that Comp B (or at least its TNT component) melts just prior to or in conjunction with detonation. The temporal window for observing any experimental signatures of this feature is exceedingly narrow, and so its practical significance is unclear. For completeness, we show the predicted $\rho-T$ phase diagram in Figure 5.

Another point of interest is the shock response of molten Comp B. In order to predict this behavior, we calculated the detonation locus centered at the melt density obtained from our inert EOS and an initial energy (E_0 in (17)) as described in the previous section. The results are shown in Figure 6. The CJ speed for molten Comp B drops by just over 1% from that of the solid to 7.76 km/s, and the detonation pressure by 3.5% to 27.9 GPa.

We collect previous measurements of the CJ state as a

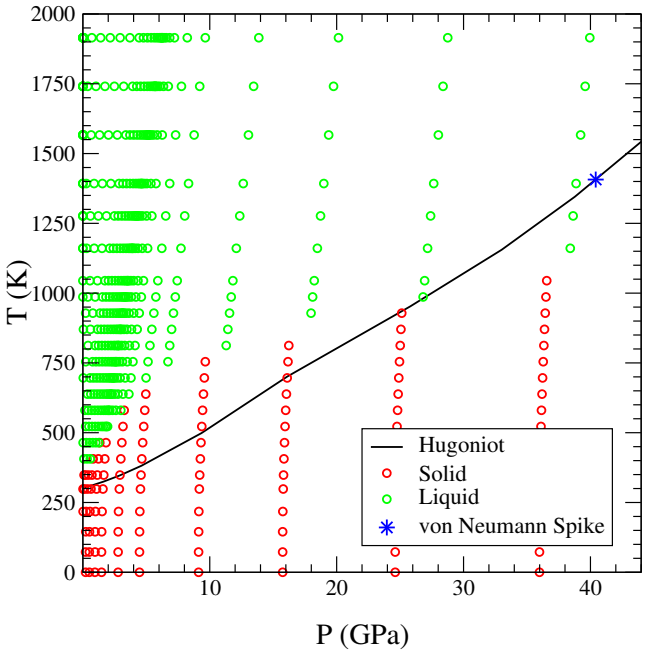

FIG. 4. The inert Hugoniot of Comp B superimposed on the $P-T$ phase diagram as predicted by SESAME 95500. Note that the von Neumann spike lies within the liquid region, based on a melt line calibrated to data for TNT alone.

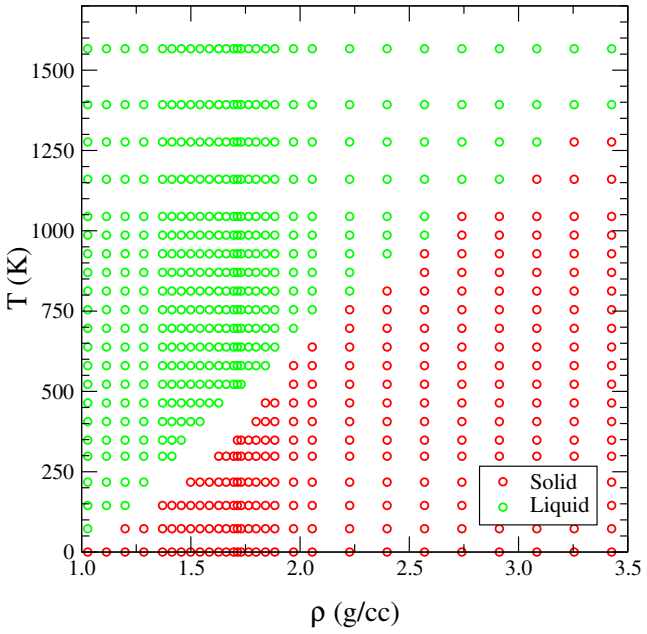

FIG. 5. The $\rho - T$ phase diagram of Comp B as predicted by SESAME 95500.

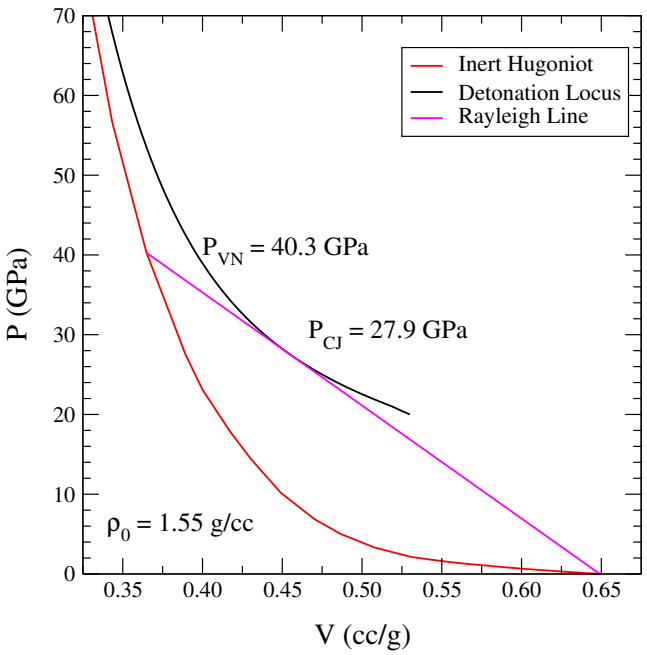

FIG. 6. The inert Hugoniot and detonation locus of molten Comp B (ρ_0=1.55 g/cc) as predicted by SESAME 95500 and chemical equilibrium calculations. Experimental uncertainties in the shock initiation data[26] are smaller than the symbol sizes. Pressures of the von Neumann spike and CJ state are also indicated.

function of composition and initial density in Table VI. Some of these figures are of dubious provenance, such as those taken from Table 8-1 of Dobratz, and rarely were experimental uncertainties reported. In Figure 7 we compare some of these results with our chemical equilibrium calculations for Comp B, LASL Comp B, and Comp B-3. Agreement is surprisingly good given the scattered and somewhat uncertain character of the data. While Ablard doesn't report a composition, his result is consistent with those of standard Comp B (as is the title of his report). Jameson, et al. call their material Comp B but report the Comp B-3 composition, consistent with our EOS result. This leaves only the data of Duff and Deal as obvious outliers.

At a couple of initial densities, there were overdriven detonation data in addition to estimates of CJ. In Figures 8 and 9 we compare `HEOS` results with those of Kineke, et al.[35] and Skidmore, et al.[29]. Our reference density for these calculations was $\rho_{\rm ref} = 1.678$ g/cc, identical to that of Kineke but slightly higher than Skidmore's ($\rho_{\rm ref} = 1.65$ g/cc. In both cases, agreement is satisfactory.

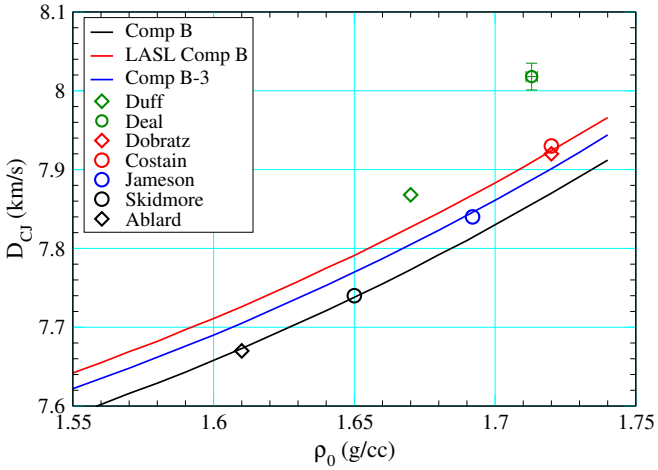

FIG. 7. Dependence of the detonation velocity D_{CJ} on the initial density as given by `HEOS` (lines) and various sources in the literature. The variation is shown for both the LASL Comp B (red line and symbols), Comp B-3 (blue line and symbols) and Comp B (black line and symbols).

IV. SUMMARY

We have compared the predictions of developmental SESAME table 95500 and chemical equilibrium calculations with data for Comp B. We hope to generate a new products table in the future.

V. ACKNOWLEDGEMENTS

This work was funded by the HE project (PL: Mark Short) of the ASC program. We thank Eric Chisolm for technical assistance.

TABLE VI. Detonation conditions for Composition B as reported by various sources. [(a)] data page [(b)] Table 8-1. Comparison with Table 8-7 suggests this may represent a JWL fit to data of unknown origin. A '-' means that the composition or type was not stated.

Source	RDX:TNT:wax	type	ρ_0(g/cc)	P_{CJ}(GPa)	D_{CJ}(km/s)
Dobratz[(a)]	63:36:1	cast	1.72	29.5	7.92
Dobratz[(b)]	Grade A	pressed	1.72	29.5	7.99
Skidmore[29]	60:40	-	1.65	25.7	7.74
Jameson[30]	60:40	cast	1.692	28.0±1.0	7.84
Duff[31]	63:37	cast	1.67	27.2±0.544	7.868
Deal[32]	64:36	cast	1.713±0.002	29.22±2.6	8.018±0.017
Ablard[33]	-	cast	1.61	-	7.67
Costain[34]	59.5:39.5:1	cast	1.72	-	7.93
HEOS	63:36:1	-	1.72	29.5	7.92
HEOS	59.5:39.5:1	-	1.713	28.9	7.86
HEOS	59.5:39.5:1	-	1.65	28.0	7.74

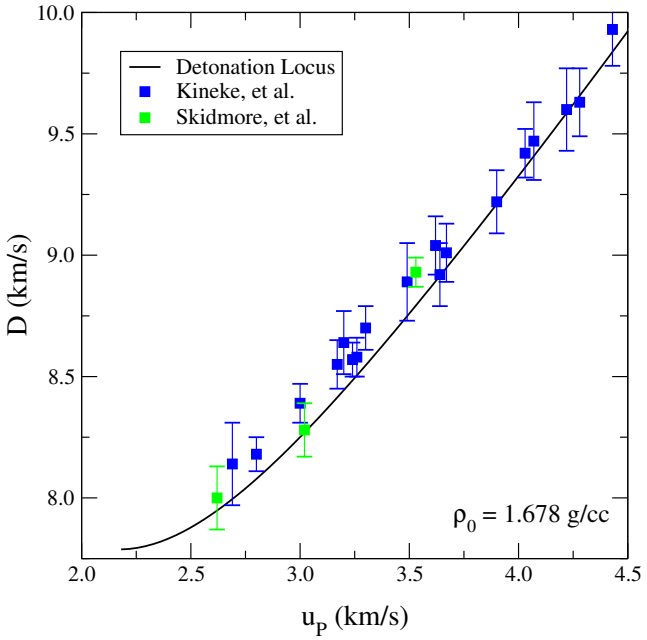

FIG. 8. The detonation locus as given by HEOS (ρ_0=1.678 g/cc) compared with the overdriven data of Kineke, et al. and Skidmore, et al. The latter were for a slightly lower initial density of ρ_0=1.65 g/cc.

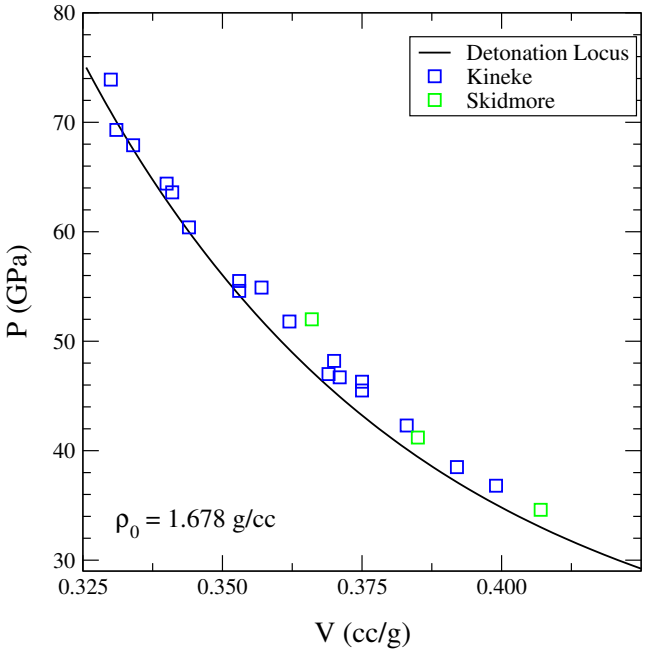

FIG. 9. The detonation locus as given by HEOS (ρ_0=1.678 g/cc) compared with the overdriven data of Kineke, et al. and Skidmore, et al. The latter were for a slightly lower initial density of ρ_0=1.65 g/cc.

[1] B. Dobratz and P. Crawford, "LLNL Explosives Handbook, Properties of Chemical Explosives and Explosive Simulants," UCRL-52997 (Lawrence Livermore National Laboratory, 1985) . The Comp B entry is on pages 19-25.

[2] S. P. Lyon and J. D. Johnson, "Sesame: The Los Alamos National Laboratory Equation of State Database," LA-UR-92-3407 (Los Alamos National Laboratory, 1992).

[3] J. Abdallah, "User's Manual for GRIZZLY," LA-10244-M (Los Alamos National Laboratory, 1984).

[4] G. I. Kerley, "User's manual for panda: A computer code for calculating equations of state," LA-8833-M (Los Alamos National Laboratory, 1981).

[5] See reference 4, section III-G.

[6] R. P. Feynman, N. Metropolis, and E. Teller, Phys. Rev. **75** (1949).

[7] R. D. Cowan and J. Ashkin, Phys. Rev. **105** (1957).

[8] Ref. 6 describes the basic algorithm for Thomas-Fermi, and Ref. 7 describes the exchange contribution. However, what is actually implemented in OpenSesame is described Appendix A of Ref. 3, which differs from Ref. 7 in its use of a zero-temperature expression for exchange at *all* temperatures.

[9] D. A. McQuarrie, *Statistical Mechanics* (University Science Books, 1976) . See Sec. 11-3.

[10] M. T. Dove, *Introduction to Lattice Dynamics* (Cambridge University Press, 1993).

[11] D. C. Wallace, *Thermodynamics of Crystals* (Dover Publications, Inc., 1972) . See pg. 52.

[12] E. D. Chisolm and D. C. Wallace, J. Phys.: Condens. Matter **13**, R739 (2001).

[13] E. D. Chisolm, "A model for liquids in wide-ranging multiphase equations of state," LA-UR-10-08329 (Los Alamos National Lab-

oratory, 2008).
[14]E. Chisolm, C. Greeff, and D. George, "Constructing Explicit Multiphase Equations of State with OpenSesame," LA-UR-05-9413 (Los Alamos National Laboratory, 2005).
[15]M. S. Shaw, Los Alamos National Laboratory, unpublished.
[16]J. S. Rowlinson and F. L. Swinton, *Liquids and Liquid Mixtures*, 3rd ed. (Butterworth Scientific, 1982) . A macroscopic treatment of ideal mixtures is given in 4.3, a microscopic one in 8.2.
[17]M. Ross, J. Comp. Phys. **71**, 1567 (1979).
[18]A. J. Stone, *The Theory of Intermolecular Forces* (Oxford University Press, 1997) . Sec. 11.1.3.
[19]M. S. Shaw, in *Proceedings of the 11th International Detonation Symposium*, ONR 33300-5 (1998) pp. 933–941.
[20]R. Menikoff, in *Shock Wave Science and Technology Reference Library*, edited by Y. Horie (Springer, 2007) Chap. 4.
[21]F. D. Murnaghan, Proc. Natl. Acad. Sci. U.S.A. **30**, 244 (1944).
[22]M. N. Pavlovskii, Sov. Phys. Solid State **13**, 741 (1971).
[23]R. G. McQueen, S. P. Marsh, J. W. Taylor, J. N. Fritz, and W. J. Carter, in *High Velocity Impact Phenomena*, edited by R. Kinslow (Academic Press, 1970) Chap. VII, pp. 293–417.
[24]M. W. Chase Jr., *NIST-JANAF Thermochemical Tables*, 4th ed., Journal of Physical and Chemical Reference Data, Monograph No. 9, Part I (American Chemical Society and American Institute of Physics, 1998).
[25]J. M. Rosen, D. V. Sickman, and W. M. Morris, "The Melting Behavior of TNT," NAVORD Report 6146 (U. S. Naval Ordnance Laboratory, 1959).
[26]L. L. Gibson, D. M. Dattelbaum, B. D. Bartram, S. A. Sheffield, R. L. Gustavsen, G. W. Brown, M. M. Sandstrom, A. M. Gi-ambra, and C. A. Handley, J. Phys.: Conf Ser. **500**, 192004 (2014).
[27]W. Fickett and W. C. Davis, *Detonation: Theory and Experiment* (Dover Publications, Inc., 1979) See Sec. 2A.
[28]D. M. Dattelbaum, R. S. Chellappa, P. R. Bowden, J. D. Coe, and M. A. Margevicius, Appl. Phys. Lett. **104**, 021911 (2014).
[29]I. C. Skidmore and S. Hart, in *Proceedings of the 4th Symposium (International) on Detonation*, ACR-126, edited by S. J. Jacobs (Office of Naval Research - Department of the Navy, Washington, D.C., 1965) pp. 47–51.
[30]R. L. Jameson and A. Hawkins, in *Proceedings of the 5th Symposium (International) on Detonation*, ACR-184, edited by S. J. Jacobs and R. Roberts (Office of Naval Research - Department of the Navy, Washington, D.C., 1970) pp. 23–29.
[31]R. E. Duff and E. Houston, J. Chem. Phys. **23** (1955).
[32]W. E. Deal, Phys. Fluids **1**, 523 (1958).
[33]J. E. Ablard, "Composition B: A Very Useful Explosive," NAVSEA-03-TR-058 (Ablard Enterprises, Inc., 1977).
[34]T. S. Costain and R. V. Motto, "The Sensitivity, Performance, and Material Properties of Some High Explosive Formulations," 4587 (Picatinny Arsenal, Dover, NJ, 1973).
[35]J. H. Kineke and C. E. West, in *Proceedings of the 5th Symposium (International) on Detonation*, ACR-184, edited by S. J. Jacobs and R. Roberts (Office of Naval Research - Department of the Navy, Washington, D.C., 1970) pp. 533–543.